J Mater Sci (2011) 46:1850–1856
DOI 10.1007/s10853-010-5012-4

Synthesis and characterization of composite membrane by deposition of acrylic acid plasma polymer onto pre-treated polyethersulfone support

Betina Villagra Di Carlo · Juan Carlos Gottifredi · Alberto Claudio Habert

Received: 20 August 2010 / Accepted: 15 October 2010 / Published online: 11 November 2010

Abstract The plasma techniques were explored to deposit a layer of hydrophilic polymer on asymmetric porous membranes used as support material. Microporous membranes were synthesized by the phase inversion technique from polyethersulfone (PES) and submitted to a surface treatment with RF-plasma of non-polymerizable gas. Carbon dioxide (CO_2) was selected to generate this plasma and to increase the surface energy. Further plasma treatment proceeded with acrylic acid (AA) in vapor phase as source for the permanent surface hydrophilic functionalization. The infrared spectra with horizontal attenuated total reflectance (HATR) show that the deposited plasma polymer provides a high concentration of carbonyl and hydroxyl groups. The hydrophilic polymer layer was evenly deposited, with good adhesion to the support, as was observed by electronic microscopy (SEM). The surface free energy (γ_S) was increased through plasma treatments and confirmed by the decrease of contact angle (θ) measurements and increase of adhesion work (W_a). The nitrogen permeability decreased 650 times; after that a dense thin film was deposited by plasma treatment during 40 min (at 5 W and 8 Pa). Final composite membranes show stability, high surface hydrophilicity, and a surface chemical nature very stable with time.

B. Villagra Di Carlo (✉) · J. C. Gottifredi
Instituto de Investigaciones para la Industria Química (INIQUI-CONICET), Facultad de Ingeniería, Universidad Nacional de Salta, Av. Bolivia 5150 c/p 4400, Salta, Argentina
e-mail: betinadicarlo@gmail.com

A. C. Habert
Programa de Engenharia Química, COPPE, Universidade Federal do Rio de Janeiro, Rio de Janeiro, Brazil

Introduction

The phase inversion technique has been widely used to synthesize anisotropic porous membranes over which plasma treatments have been applied [1], modified with hydrophilic polymers [2] or grafting [3], aiming at the fabrication of suitable membranes for microfiltration [4], ultrafiltration [5], or as support material in the production of composite membranes for reverse osmosis and pervaporation [6]. Plasma is a gas state of matter which includes a variety of neutral and ionized species such as molecules, atoms, electrons, ions, free radicals, and photons, which can be used to modify and functionalize the materials surface, as porous and dense polymer membranes for the enhancing of their separation properties. Treatments with radio frequency plasma at low pressure were successful in generating functional groups [7], surface crosslinking [8], pore size reduction [9], chemical grafting [10], thin organic layer deposition [11] but also, under certain conditions, severe ablation. To achieve required properties a number of operational parameters must be selected to modify a specific polymer membrane, such as the nature of the gas or the organic vapor plasma precursor (polymerizable or non-polymerizable), input flow rate into the reactor to sustain an adequate pressure, discharge power to control the transferred energy to species, and exposure time of the polymeric substrate [12]. Plasma generated with gaseous organic monomers can polymerize and crosslink on the exposed surface, forming a dense polymeric coating with specific characteristics [13]. Plasmas modify surface physical–chemical properties (hydrophilicity, ruggedness, adherence, chemical composition, and morphology) keeping however bulk properties unaltered [6]. Potential applications have been reported with these treated membranes by plasma techniques: separation processes [14],

ultrafiltration fouling reduction [15], and biomedical applications (particularly increasing biocompatibility) [16]. Main advantages of plasma technology are also pointed out: speed, simplicity, versatility, a reduced quantity of chemical compound requirements during plasma processing, and a small waste production, consequently low environmental impact [17].

The scope of this study was to synthesize a composite membrane exploring plasma techniques. Polyethersulfone (PES) was selected as the starting bulk polymer due to its excellent properties: mechanical, structural, and permeability. Bulk PES was dissolved in dimethylformamide to prepare microporous membranes by phase inversion technique. To get a suitable asymmetric porous structure, polyvinyl-pyrrolidone was added to the casting solution. The obtained membranes were then treated with non-polymerizable CO_2 plasma to clean and activate the surface.

In a second stage, an acrylic acid (AA) layer produced by controlled plasma polymerization in situ was deposited over the previous activated surface. Surface chemical nature was studied using FTIR-HATR. Surface physicochemical properties were analyzed through measurements of θ (contact angle) and estimation of γ_S (surface free energy) and W_a (adhesion work). Cross-section and surface morphologies were investigated by SEM. Finally, pure gas permeation experiments (N_2 and CO_2) were performed to determine components' permeability and ideal selectivity.

Experimental

Materials

Polyethersulfone (Ultrason E6020) and polyvinyl-pyrrolidone (PVP, Mw $\sim$ 40,000 g/mol) were supplied by Basf and Sigma, respectively. AA (Analyticals-Carlo Erba), with 0.05% of hydroquinone metal ether as stabilizer, was chosen as plasma monomer, and *N*,*N*-dimethyl formamide (DFM, Merck) was added as solvent to prepare membrane casting solutions. Distilled water was selected as external coagulant for PES membranes. All products were of analytical grade and used without further purification. Carbon dioxide, 99.9%, and nitrogen, 99.9% were provided by Praxair.

Porous membrane synthesis

The phase inversion by immersion in a non solvent technique was selected to prepare asymmetric membranes. Polymers were dried in a stove at 60 °C for a minimum period of 24 h. Casting solution composition was 15% PES, 7.5% PVP, and 77.5% DMF in weight [18] and was spread on a glass plate, allowing solvent evaporation for 60 s. A 50% vol water–DMF solution was used to precipitate the porous polymeric structure. Membranes were washed three times with distilled water and then kept immersed in a water bath at 60 °C for 12 h to remove remaining sorbed solvent. A final washing process in two stages (ethanol followed by *n*-hexane) was carried out to insure the conservation of membrane morphology in the next step. The membranes were then dried at room temperature and stored under controlled dry atmosphere.

Membranes plasma pre-treatment

Porous membranes were set in the center of plasma reactor chamber (15 cm in diameter and 15 cm in depth, Harrick inductive Plasma 8–12 MHz). Before plasma treatment, membranes were kept under vacuum during 10 min to insure complete solid drying. Then, the reactor chamber was purged twice with CO_2 (precursor gas) at room temperature. Operating conditions of CO_2 plasma pre-treatment were 106 Pa chamber pressure and 7.2 W discharging power of the source. A mechanical vacuum pump was continuously operated to achieve and maintain reactor pressure during the plasma treatment. The low applied power reduces damage on membrane surface due to energetic plasma species [19]. Exposure time was 5 min after a series of experiments to achieve an appreciable modification on the surface hydrophilicity.

Plasma polymer deposition

The previously treated polymeric supports were exposed to plasma polymerization in a capacitive reactor. AA vapor was fed at 8 Pa, during 20 and 40 min. RF discharge and power were 13.56 MHz and 5 W, respectively [20].

Characterization

The polymeric membranes cross-section and surface morphologies were investigated by Scanning Electronic Microscopy (SEM, Jeol JSM-6480 LV). Membrane samples were frozen and broken in liquid N_2 for cross-sectional imaging and further gold sputter-coated to prevent charging effects. Images were taken at 15 and 10 kV setting with 270×, 10 k×, and 16 k× magnification.

The surface properties were followed measuring water/membrane contact angle under atmospheric conditions. A distilled water drop (10 μL) was poured on the membrane surface and contact angle was determined with a goniometer (Ramé-Hart, with DROPimage). Equipment software estimates surface free energy (mJ m^{-2}) from measured contact angle and surface tension of water by means of an iterative procedure proposed by Neumann (Eq. 1) [21]. Adhesion Work (mJ m^{-2}) was calculated using a

combination of the Young and Dupré equations [22]. Final reported average contact angle for each membrane is the average measurements on five different locations for each membrane surface; the maximum dispersion was ±0.5° in the measured values.

$$\cos\theta = -1 + 2\sqrt{\frac{\gamma_S}{\gamma_L}}\, e^{-\beta(\gamma_L-\gamma_S)^2} \quad (1)$$

where θ (°) is the contact angle, γ_L (mJ m^{-2}) is the liquid tension, γ_S (mJ m^{-2}) is the surface free energy, and β is a parameter determined from experimental data, $\beta = 0.0001247$ (m^2 mJ^{-1})^2.

Surface chemical nature was studied using Fourier transform infrared spectroscopy (FTIR, Perkin-Elmer, Spectrum GX) with horizontal attenuated total reflectance (HATR). The ZnSe crystal at a nominal incident angle of 45° yielded 12 internal reflections on each sample. All spectra were scanned 12 times, between 4000 and 630 cm^{-1}, under 4 cm^{-1} resolution. Penetration depth of beam, with this analysis, depends not only on wavelength but also on the incidence angle [23].

Permeation properties were studied in a standard equipment at room temperature [24]. Effective permeability coefficients of pure gases (CO_2, N_2) were determined under steady state conditions from the slope of the plot of permeate flux (per unit area of membrane) as function of the pressure drop across the membrane (Eq. 2) [25]. The membrane area of the flow cell in all experiments was 8.55 cm^2, and all reported fluxes are always expressed in standard conditions (STP, 273 K, 1 atm.).

$$\frac{Q}{A} = P\Delta P \quad (2)$$

where Q [cm^3 (STP)/s] is the gas permeation flux through the membrane, A (cm^2) is the effective membrane area, P [cm^3 (STP)/cm^2 s cmHg] is the effective permeability coefficient, and ΔP (cmHg) is the differential across the membrane. The total mass transfer resistance, R_t [cmHg s/cm^3 (STP)], across the membrane, was calculated from Eq. 3 [26]:

$$R_t = \frac{1}{PA} \quad (3)$$

The separation factor, α, is estimated from Eq. 4 [25]:

$$\alpha_{CO_2/N_2} = \frac{P_{CO_2}}{P_{N_2}} \quad (4)$$

Results and discussion

Morphology

SEM of the cross-section of the PES base membrane shows the asymmetric structure of the synthesized porous support layer (Fig. 1a). Thickness is approximately 280 μm. Toward the bottom face of the membrane a finger structure, formed by interconnected macroporous of growing diameter from 2.5 to 75 μm, can also be observed.

Figure 1b shows a SEM microphotograph of the composite membrane (PESM40) cross-section. A very thin film (~300 nm) of plasma polymer, after the two stage plasma treatments, can be clearly noticed. A truly composite membrane has been obtained with a non-porous skin deposited onto the PES porous membrane (which surface was previously activated by a CO_2 plasma). One can observe a spongy structure region of approximately 3–5 μm below the plasma layer, with polymeric nodular aggregates and pores belonging to the support layer [27].

A closer look in Fig. 1c shows a compact morphological structure of the skin which largely differs to traditional coating with conventional bulk polymers. The resulting top layer can be characterized by being non-porous, well adhered, uniform, and stable in water and ethanol at room temperature.

Hydrophilicity, surface free energy, and adhesion work

Contact angle measurement is widely used to establish the hydrophilic nature of surfaces. The θ value of 64° observed with the PES support membranes is quite lower than the 82° value reported for dense PES (Table 1). This reduction is usually explained in terms of combined effects of porosity, roughness, and the hydrophilic additive remains (PVP) trapped in the polymeric matrix.

Plasma CO_2 treatment (7.2 W, 160 Pa, 5 min) cleans and activates the substrate membrane surface, removing weakly bound surface material and creating active sites. It leads to an important decrease of θ value to 33°, while increasing the surface free energy and adhesion work, as it can be seen in Table 1. After 5 min of plasma treatment (CO_2, 7.2 W, 160 Pa), the contact angle changes are less pronounced (Fig. 2). A plasma treatment for prolonged time can cause significant damage to membrane surface [28]. Possibly, under plasma treatment, surface chemical nature of PES membrane is modified due to the formation of active groups such as carboxylic acid, ketone/aldehyde, and ester [29]. Those probably contribute to the initiation of the polymerization with the hydrophilic monomer. Then the plasma treatment with AA vapor (5 W, 8 Pa, 40 min) produces a stable top layer with a 27° θ value (Table 1). Modified membranes after AA plasma exposure for 20 min (5 W, 8 Pa) have the same contact angle value (27°), probably there is plasma polymer on the surface, although is not observed by SEM. It should be stressed that application of a conventional poly(acrylic acid) (PAA) coating in two stages on PES-synthesized membranes leads to contact angle of 49°. The hydrophilicity of the plasma

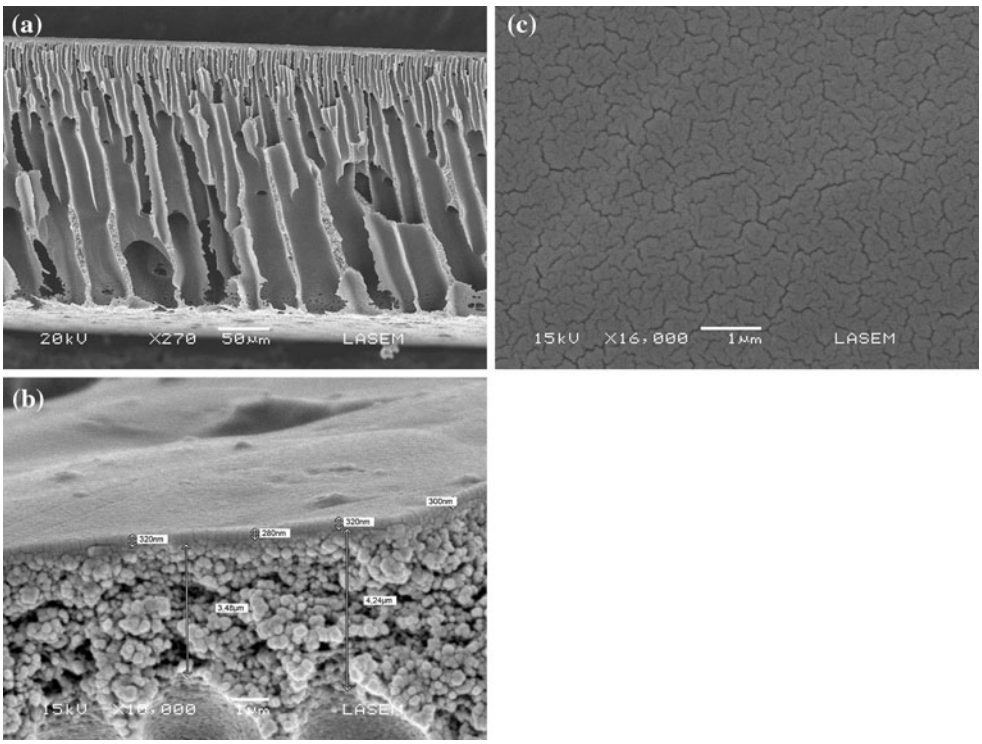

Fig. 1 **a** Cross-section of PES support membrane (magnification: 270×), **b** cross-section of composite membrane AA plasma/PES (PESM40, magnification: 10 k×), **c** surface of composite PESM40 membrane (magnification: 16 k×)

Table 1 Surface physicochemical properties of membranes

The bold values correspond to the initial support membrane and the final composite membrane (coated by plasma deposition)

Membrane	Contact angle (θ) (°)	Superficial energy (γ_S) (mJ/m^2)	Adhesion work (W_a) (mJ/m^2)
PES (dense)	82	33.67	81.81
PES (porous)	**64**	**45.64**	**107.73**
PES + CO_2 plasma	33	62.78	133.83
PES + AA plasma	**27**	**65.78**	**137.14**
PES + PAA	49	54.35	119.84

polymer is larger than that of the one observed with the PAA conventional polymer (Table 1).

As the plasma CO_2 treatment produces a remarkable increase of surface hydrophilicity, nevertheless an aging process occurs (Fig. 3) [28, 30]. These changes with time can be due to chemical arrangement to minimize the surface free energy. On the other hand, the deposition of a film through AA plasma polymerization has important effects, for the increase and the stabilization of the induced hydrophilicity on the resulting membrane surface. Thus the plasma coating is not subject to aging (Fig. 3) stored in ambient conditions.

Surface chemical composition

FT-IR/HATR was used to identify functional groups of the plasma polymer film deposited over PES-synthesized membrane after being activated with CO_2 plasma. Depth of penetration of FT-IR/HATR beam (dp) changes with wavelength [23]. If dp is larger than the deposited top layer thickness, then the chemical groups belonging to the PES support membrane will also be detected [16]. Observation of the composite PESM40 membrane spectrum is shown to detect the presence of chemical groups. From Fig. 4, stretching of O–H group (3495 cm^{-1}), C–H (2950 cm^{-1}), carbonyl –C=O (1710 cm^{-1}), H–C–H (1459 cm^{-1}), plane bending C–O–H (1400–1200 cm^{-1}), and bending out of plane =C–H (800 cm^{-1}) can be observed [6, 10, 16, 31]. Also, it is inferred that the deposited film retains a high grade of AA monomer functionalities (1760 cm^{-1}) and AA dimer (1710 cm^{-1}), revealing that AA monomer structure was preserved under power and pressure reaction conditions. The C=O peak is wide and not symmetrical, suggesting too a contribution of ester groups (1735 cm^{-1}).

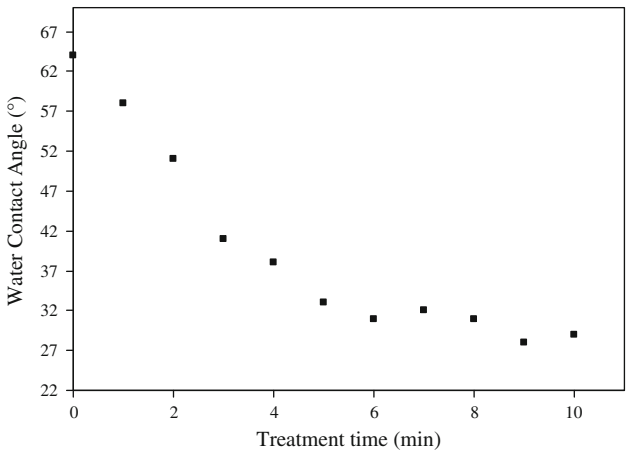

Fig. 2 Dependence of water contact angle as a function of the plasma treatment time on the support membrane surface (PES, CO_2, 7.2 W, 160 Pa)

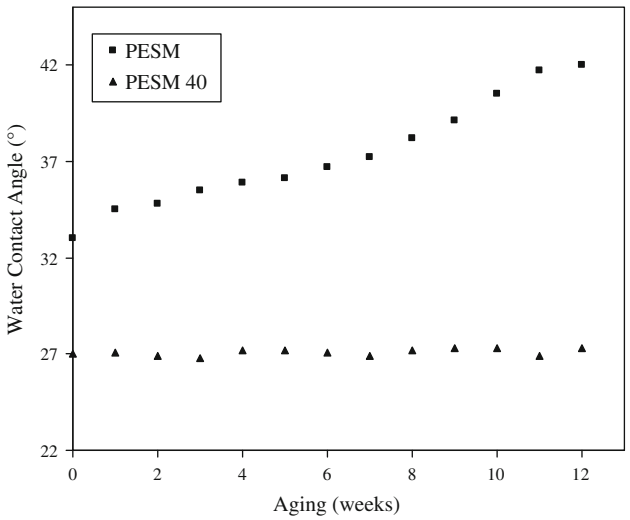

Fig. 3 Water contact angle as a function of the aging on the treated substrate membrane surface (PESM, CO_2, 7.2 W, 160 Pa, 5 min) and on the composite membrane surface (PESM40, AA, 5 W, 8 Pa, 40 min)

The peak located at 1640 cm^{-1} in the PES spectrum (Fig. 4) can be assigned to the presence of C=C–N group of the hydrophilic additive (PVP) remained trapped in the polymeric matrix of PES support membranes [32].

When the PES membrane and modified surface membrane spectra are compared (Fig. 4) it can be seen that, within the range 1600–600 cm^{-1}, species of unmodified PES membrane are still noticed on deposited AA plasma membrane. Under these conditions, beam penetration depth is always larger than the film thickness, revealing therefore the chemical structure located below the deposited skin.

The peak located at 800 cm^{-1} in the PESM40 spectrum is remarkably important when compared with PAA bulk polymer spectrum (Fig. 5). It should be noticed that

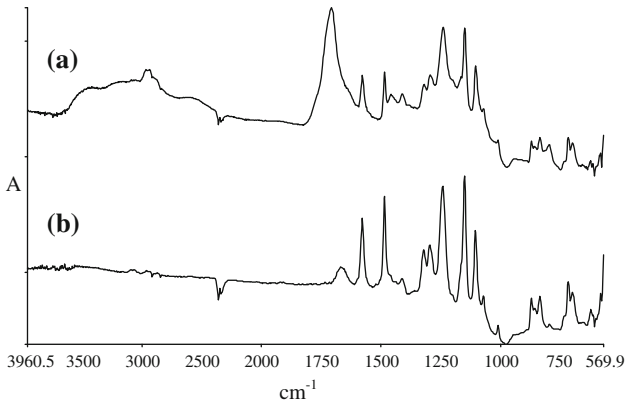

Fig. 4 FT-IR/HATR spectra of (*a*) AA plasma/PES composite membranes (PESM40) and (*b*) PES support membranes

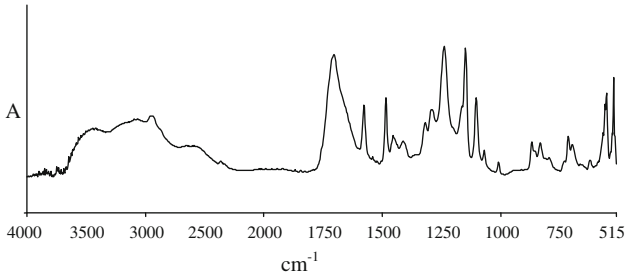

Fig. 5 FT-IR/HATR spectra of PAA/PES composite membrane (PES + coated PAA conventional polymer)

penetration depth is approximately 2.8 μm at this wavenumber, a large value when compared with 0.3 μm of the AA plasma skin thickness. Therefore, the absorbance signal at this position refers 10% to the AA plasma polymer and 90% to the PES substrate. From the literature [16] this peak can be assigned to the presence of =C–H group. Possibly, the formed polymer structure on the functionalized porous surface is the result of an incomplete polymerization.

The absorbance ratio of C=O with regard to both C–H and O–H groups are larger in the plasma polymer (Fig. 4) than that in the conventional PAA (Fig. 5). This is probably the reason of the larger hydrophilicity in the plasma polymer as was demonstrated from the values of contact angle reported in Table 1.

When a polymeric membrane is exposed to action of plasma a number of chemical reactions could take place. Under these conditions competitive mechanisms involving ablation and deposition are established. Depending upon the applied power, pressure, reaction time exposure, chemical vapor, and support membrane composition, a given mechanism could become dominant.

On the other hand, the plasma CO_2 treatment produced surface functional groups that can be conceived as active

sites for reactions. When AA monomer is sorbed on any of these sites a polymerization reaction could start. Possibly, the sorbed activated monomer species acts as a catalyst by reducing the activation energy for this initial step of reaction.

Assuming several steps for the formation of the plasma polymer, functionalization and ablation of the exposed surface (of PES) will be the most important processes in the first stages. Then the polymerization reaction will start while substrate and deposited plasma polymer will be etched and grafted simultaneously. The layer of plasma polymer in formation incorporates molecules of monomer, dimer, oligomer, and fragments. On the final stages, the deposited plasma film on the activated PES membrane surface will be affected by a combination of the appointed reactions above.

Permeability

The gas permeability of PES membranes can be modified with plasma treatments with both non-polymerizable gas and polymerizable vapors. The effects of treatment times and plasma procedures, on gas permeability of pure gases through modified membranes, were therefore investigated.

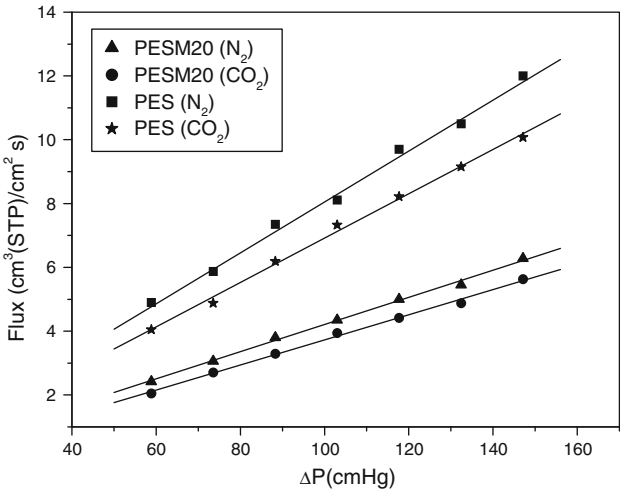

Fig. 6 Permeabilities of pure gaseous compounds (N_2 and CO_2) for the PES support membranes and the AA plasma/PES composite membranes (PESM20, 5 W, 8 Pa, 20 min)

In Fig. 6 fluxes of both pure gaseous compounds (N_2 and CO_2) are shown as function of the driving force. True linear relationships allow an estimation of permeabilities.

The pure gas permeability through the originally microporous PES membranes shows high flux values for both N_2 and CO_2. Assuming a Knudsen transport mechanism as dominant, the ratio of CO_2 to N_2 permeabilities (α_{CO_2/N_2}) will be in close agreement with Graham's diffusion law prediction [33]. In fact, as is shown in Table 2, α_{CO_2/N_2} for unmodified PES membranes is found 0.87 as estimated by the square root of the inverse ratio of CO_2/N_2 molecular weights (Eq. 5).

$$\alpha_{CO_2/N_2} = \sqrt{\frac{M_{N_2}}{M_{CO_2}}} = \sqrt{\frac{28}{44}} = 0.80 \quad (5)$$

The plasma treatment with non-polymerizable gas (CO_2) of the support membrane slightly increased the permeabilities (see Table 2). Probably due to surface etching, while transport mechanism is apparently maintained [31].

It is interesting to point out that the permeation behavior of the composite membrane PESM20 (AA, 5 W, 8 Pa, 20 min) is similar to the porous support. Although permeabilities of both gases decrease 51%, ideal selectivity does not change (see Table 2).

Possibly with 20 min of AA plasma treatment a complete coating of plasma polymer was not yet formed. Nevertheless, surface pore diameter may have already been reduced, which explains the noticeable flux decrease, although controlled by a Knudsen transport. As coating occurs, a probable surface etching is competing.

As is shown in Fig. 7, same gas permeabilities through modified PES membranes are strongly affected by two stages of plasma treatment. AA deposition produces, as is expected, permeability decrease and α increase.

The plasma polymer deposition on the PES-activated surface increases total mass transfer resistance up to 650 times for the case of the maximum exposure time of 40 min and N_2 permeation (see Table 2). At the same time, mass transport within the deposited AA polymer is no

Table 2 Permeability P [cm^3 (STP)/cm^2 s cmHg], ideal selectivity $\alpha(CO_2/N_2)$, and total gas permeation resistance R_t [cmHg s/cm^3 (STP)] for N_2

Membrane	P_{N_2}	P_{CO_2}	$\alpha_{(CO_2/N_2)}$	R_t (N_2)
PES (porous)	**8.04E−2**	**6.96E−2**	**0.87**	**1.45**
PES + CO_2 plasma	8.21E−2	7.44E−2	0.91	1.42
PES + AA plasma (20 min)	4.23E−2	3.76E−2	0.89	2.76
PES + AA plasma (40 min)	**1.26E−4**	**1.63E−4**	**1.29**	**928.24**

The bold values correspond to the initial support membrane and the final composite membrane (coated by plasma deposition)

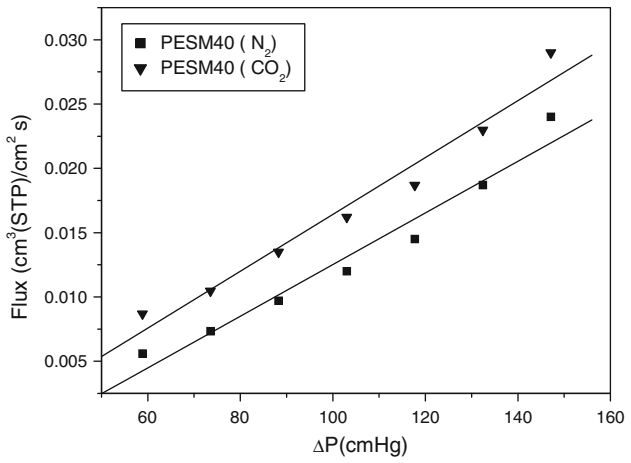

Fig. 7 Permeabilities of pure gaseous compounds (N_2 and CO_2) for the AA plasma/PES composite membranes (PESM40)

longer governed by pure diffusional phenomenon. Rather a simultaneous sorption–diffusion mechanism becomes dominant while the PES support membrane resistance turns negligible.

As polar CO_2 is more soluble than N_2, ideal selectivity is now reversed. A stable plasma film on the PESM surface was only observed in the case of PESM40 (Fig. 1b). Moreover the resulting chemical structure of this skin is similar regarding the presence of functional groups (O–H and C=O) in the PAA conventional polymer, but with different relationships [16]. The strong evidence of C=O presence could be a suitable explanation for a greater affinity of CO_2 in comparison with N_2.

Conclusions

Morphological and transport properties of PES-synthesized membranes resulted in suitable support to produce composite membranes. Plasma treatment, under CO_2 atmosphere, revealed to be an effective technique to modify hydrophobic surface properties of PES porous membranes. Successful deposition of films with thickness of approximately 300 nm from AA vapor plasma (5 W, 8 Pa, 40 min) can be obtained and well characterized. The structure of the organic monomer (AA) was preserved under the used plasma polymerization conditions and increased the content of hydrophilic groups comparing with the PAA conventional polymer. Contact angle confirms the high hydrophilic character of plasma skin and its stability with time. Pure N_2 and CO_2 gas permeabilities, through resulting composite membranes (PESM40), no longer obeyed Graham's law. Total gas permeation resistance (N_2) was found 650 times smaller than corresponding values observed with PES support membranes.

Acknowledgements The authors appreciate the support of ANPCyT, SECyT, CAPES, and CIUNSA. Betina Villagra Di Carlo would like to thank ANPCyT and CONICET for scholarship grant.

References

1. Lee KR, Teng MY, Lee HH, Lai JY (2000) J Memb Sci 164:13
2. Ma X, Su Y, Sun Q, Wang Y, Jiang Z (2007) J Memb Sci 300:71
3. Belfer S, Fainchtain R, Purinson Y, Kedem O (2000) J Memb Sci 172:113
4. Deng B, Li J, Hou Z, Yao S, Shi L, Liang G, Sheng K (2008) Radiat Phys Chem 77:898
5. Idris A, Zain NM, Noordin MY (2007) Desalination 207:324
6. Kim H, Kim S (2001) J Memb Sci 190:21
7. Su CY, Lin CK, Lin CR, Lin CH (2006) Surf Coat Technol 200:3380
8. Upadhyay DJ, Bhat NV (2004) J Memb Sci 239:255
9. Tran DT, Mori S, Suzuki M (2008) Thin Solid Films 516:4384
10. Oehr C, Muller M, Elkin B, Hegemann D, Vohrer U (1999) Surf Coat Technol 116–119:25
11. Dayss E, Leps G, Meinhardt J (1999) Surf Coat Technol 116–119:986
12. Kelly JM, Short RD, Alexander MR (2003) Polymer 44:3173
13. Yasuda H (1985) Plasma polymerization. Academic Press, New York
14. Shi FF (1996) Review. Surf Coat Technol 82:1
15. Wavhal DS, Fisher ER (2002) J Memb Sci 209:255
16. Sciarratta V, Vohrer U, Hegemann D, Müller M, Oehr C (2003) Surf Coat Technol 174–175:805
17. Tran ND, Dutta NK, Choudhury NR (2005) Thin Solid Films 491:123
18. Pereira CC, Nobrega R, Borges CP (2001) J Memb Sci 192:11
19. Wavhal DS, Fisher ER (2005) Desalination 172:189
20. Weibel DE, Vilani C, Habert AC, Achete CA (2007) J Memb Sci 293:124
21. Kwok DY, Neumann AW (2000) Colloids Surf A Physicochem Eng Asp 161:31
22. Tabaliov NA, Svirachev DM (2007) Appl Surf Sci 253:4242
23. Klages CP, Grishin A (2008) Plasma Process Polym 5:359
24. Chapman CL, Bhattachary D, Eberhart RC, Timmons RB, Chuong CJ (2008) J Memb Sci 318:137
25. Lopez JL, Matson SL, Marchese J, Quinn JA (1986) J Memb Sci 27:301
26. Matson SL, Lopez J, Quinn JA (1983) Chem Eng Sci 38:503
27. Khulbe KC, Feng CY, Matsuura T (2008) Synthetic polymeric membranes: characterization by atomic force microscopy. Springer-Verlag, Berlin Heidelberg
28. Gancarz I, Pozniak G, Bryjak M (1999) Eur Polym J 35:1419
29. Wavhal DS, Fisher ER (2002) J Polym Sci B Polym Phys 40:2473
30. Hegemann D, Brunner H, Oehr C (2003) Nucl Instrum Methods Phys Res B 208:281
31. Tran T, Mori S, Suzuki M (2007) Thin Solid Films 515:4148
32. Solak EK, Asman G, Camurlu P, Sanli O (2008) Vacuum 82:579
33. Baker RW (2004) Membrane technology and applications. Wiley, Chichester